

# In situ Synchrotron IR Microspectroscopy of CO<sub>2</sub> Adsorption on Single Crystals of the Functionalized MOF Sc<sub>2</sub>(BDC-NH<sub>2</sub>)<sub>3</sub>\*\*

Alex Greenaway, Berenice Gonzalez-Santiago, Paul M. Donaldson, Mark D. Frogley, Gianfelice Cinque, Jorge Sotelo, Stephen Moggach, Elenica Shiko, Stefano Brandani, Russell F. Howe,\* and Paul A. Wright\*

**Abstract:** Synchrotron radiation (SR) IR microspectroscopy has enabled determination of the thermodynamics, kinetics, and molecular orientation of CO<sub>2</sub> adsorbed in single microcrystals of a functionalized metal–organic framework (MOF) under conditions relevant to carbon capture from flue gases. Single crystals of the small-pore MOF, Sc<sub>2</sub>(BDC-NH<sub>2</sub>)<sub>3</sub>, (BDC-NH<sub>2</sub> = 2-amino-1,4-benzenedicarboxylate), with well-defined crystal form have been investigated during CO<sub>2</sub> uptake at partial pressures of 0.025–0.2 bar at 298–373 K. The enthalpy and diffusivity of adsorption determined from individual single crystals are consistent with values obtained from measurements on bulk samples. The brilliant SR IR source permits rapid collection of polarized spectra. Strong variations in absorbance of the symmetric stretch of the NH<sub>2</sub> groups of the MOF and the asymmetric stretch of the adsorbed CO<sub>2</sub> at different orientations of the crystals relative to the polarized IR light show that CO<sub>2</sub> molecules align along channels in the MOF.

MOFs exhibit properties that make them strong candidates for post combustion carbon capture, including acceptable uptakes of CO<sub>2</sub> and high selectivity, regenerability, and stability to water.<sup>[1]</sup> The conventional approach to assess a potential sorbent is to acquire adsorption isotherms at relevant temperatures. However, this can be slow, even when only single component adsorption is performed—the collection of multicomponent isotherms is much more demanding.<sup>[2]</sup>

IR spectroscopy is widely used to follow the uptake of CO<sub>2</sub> on powdered samples of microporous sorbents, where

absorption frequencies and intensities give information on the type and amount of adsorption and variable temperature studies give enthalpies and entropies of uptake that can be compared to values determined by other methods, such as analysis of isotherms or calorimetry.<sup>[3–6]</sup> Where single crystals are available, IR microspectroscopic analysis (combined optical microscopy and IR spectroscopy) has been used for the determination of concentration-dependent diffusion parameters of hydrocarbons.<sup>[7,8]</sup> Here, we have used for the first time synchrotron-based single-microcrystal Fourier transform IR spectroscopy coupled with optical microscopy to quantify the performance of an amino-functionalized MOF, Sc<sub>2</sub>(BDC-NH<sub>2</sub>)<sub>3</sub>, as a carbon capture sorbent, through measurement of the heat of adsorption and the rate of desorption. This MOF shows enhanced uptake of CO<sub>2</sub> over its unfunctionalized variant<sup>[9]</sup> and the amino groups in the MOF act as an internal reference for IR analysis. Furthermore, we make use of single-crystal microspectroscopy with polarized IR light to determine the orientation of adsorbed CO<sub>2</sub> molecules. For crystalline samples in which the orientation of the lattice can be associated with the external morphology of the crystal, single-crystal-polarized IR spectroscopy is able to determine the orientation of molecules adsorbed within the micropores.<sup>[10]</sup> Synchrotron IR radiation (which gives an about 100-fold increase in photon flux density over Global laboratory sources) yields a large improvement in the signal-to-noise ratio so that high quality direction-dependent polarized IR spectra can be measured for anisotropic

[\*] Dr. A. Greenaway, B. Gonzalez-Santiago, Prof. P. A. Wright  
EaStCHEM School of Chemistry, Purdie Building  
St Andrews, KY16 9ST (UK)  
E-mail: paw2@st-andrews.ac.uk


Prof. R. F. Howe  
Department of Chemistry, University of Aberdeen  
Meston Buildings, King's College  
Aberdeen, AB24 3UE (UK)  
E-mail: r.howe@adbn.ac.uk


J. Sotelo, Dr. S. Moggach  
EaStCHEM School of Chemistry, Joseph Black Building  
West Mains Road, Edinburgh, EH9 3JJ (UK)

Dr. P. M. Donaldson, Dr. M. D. Frogley, Dr. G. Cinque  
Diamond Light Source  
Harwell Science and Innovation Campus  
Didcot, OX11 0DE (UK)

E. Shiko, Prof. S. Brandani  
School of Engineering, University of Edinburgh  
Sanderson Building, The King's Buildings  
Mayfield Road Edinburgh EH9 3JL (UK)

[\*\*] We thank the EPSRC (AMPgas, EP/J02077X/1; AG, PAW, ES, SB), CONACYT, Mexico (BG-S) and the University of Edinburgh (JS) for funding, Dr. Stephen Thompson for assistance at I11 and Diamond Light Source for beam time on stations B22 (Expts. SM8875-1, SM10014-1) and I11 (EE9027-1). MOF = metal–organic framework, BDC-NH<sub>2</sub> = 2-amino-1,4-benzenedicarboxylate.

 Supporting information for this article including details of the in situ IR experiments, single-crystal and powder X-ray diffraction, zero length column chromatography, and gravimetric analysis are given in the Supporting Information is available on the WWW under <http://dx.doi.org/10.1002/anie.201408369>.

 © 2014 The Authors. Published by Wiley-VCH Verlag GmbH & Co. KGaA. This is an open access article under the terms of the Creative Commons Attribution License, which permits use, distribution and reproduction in any medium, provided the original work is properly cited.

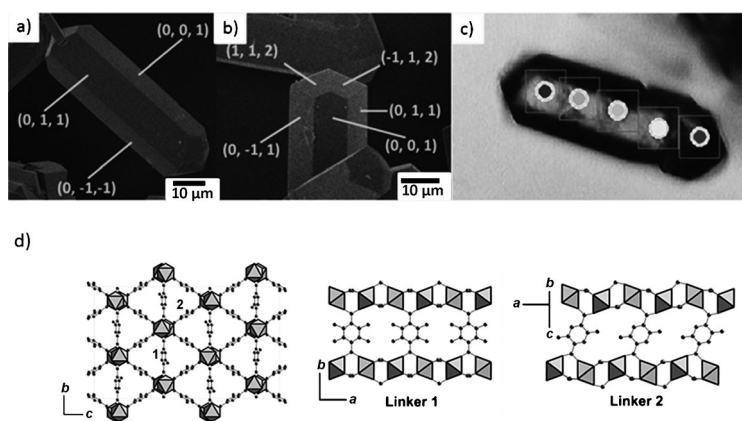


**Figure 1.** a,b) SEM of  $\text{Sc}_2(\text{BDC-NH}_2)_3$  crystals with face indices marked ( $10\ \mu\text{m}$  scale bars shown), c) optical micrograph showing sites selected on the same crystal for IR analysis, (boxes represent  $10 \times 10\ \mu\text{m}$  area from which spectra are collected). d) Framework structure of  $\text{Sc}_2(\text{BDC-NH}_2)_3$  ( $\text{ScO}_6$  gray octahedra, C and N atoms shown as spheres (all possible N atom positions included and H omitted).

materials. The technique has been exploited to identify the orientation of adsorbed *para*-xylene molecules in SAPO-5<sup>[11]</sup> and recently Eschenroeder et al. used it to determine the orientation of metal–amine complex templates in the zeotype STA-7.<sup>[12]</sup>

Microcrystals ( $80 \times 20 \times 20\ \mu\text{m}^3$ ) of  $\text{Sc}_2(\text{BDC-NH}_2)_3$  were synthesized by a solvothermal technique (see Figure 1 a–c and the Supporting Information). Single-crystal X-ray diffraction indicated the crystals have orthorhombic *Fddd* symmetry. The most strongly developed faces of the crystals were indexed to be of the forms  $\{011\}$  and  $\{001\}$ , which are indicated on scanning electron micrographs in Figure 1 a (see also Figures S2.1 and S2.2 in the Supporting Information). The long axis of the crystals is parallel to the *a* axis, which corresponds to the channel axis. The structure (Figure 1 d) is built from rows of isolated  $\text{ScO}_6$  octahedra running along the *a* axis, linked by bridging carboxylate groups. This results in a series of triangular channels around  $4\ \text{\AA}$  in free diameter, bounded by amino-terephthalate groups. There are two inequivalent terephthalate linkers in the structure, one disordered over two positions close to parallel to the *xy* plane and with its  $\text{NH}_2$  group statistically disordered over four positions (linker 1), the other inclined to the *yz* plane, and with its  $\text{NH}_2$  group disordered over two positions (linker 2), with the C–N bond close to parallel to the channel axis.

In situ PXRD at 298–373 K and 0.1 bar  $\text{CO}_2$  confirmed that the structure remains orthorhombic, with very small changes in the cell parameters (see the Supporting Information). For the FTIR microspectroscopy,  $\text{Sc}_2(\text{BDC-NH}_2)_3$  crystals were loaded into a Linkam cell (path length ca. 10 mm) and this was mounted within an Bruker Hyperion 3000 IR microscope coupled to a Vertex 80 V interferometer. It was possible to identify the morphology of the crystals optically and so to determine the orientation of individual crystals. The cell allows for in situ examination under controlled gas compositions and temperature by optical microscopy and IR microspectroscopy.

The first set of experiments investigated the kinetics and thermodynamics of  $\text{CO}_2$  adsorption on single crystals of  $\text{Sc}_2(\text{BDC-NH}_2)_3$  under a gas flow of 10%  $\text{CO}_2$  in helium at temperatures relevant to temperature swing adsorption processes. Sites were selected on crystals under the microscope, bearing in mind that the incident beam size giving spectra with good signal-to-noise ratio (above 1000) was approximately  $10 \times 10\ \mu\text{m}^2$ . MicroFTIR spectra were measured in transmission using a  $15 \times$  objective/condenser with 512 scans (80 s) per point, at  $2\ \text{cm}^{-1}$  resolution. More than 20 sites were chosen both on different crystals and also on the same crystal (Figure 1 c). Spectra were taken using non-polarized IR radiation at 298 K on crystals pre-heated to 400 K, all in a dry He flow. The spectra were of such good quality that the asymmetric and symmetric  $\text{NH}_2$  stretches were clearly visible, at  $3513$  and  $3396\ \text{cm}^{-1}$  respectively. Switching the gas flow to 10%  $\text{CO}_2$  in He enabled spectra to be measured in the presence of gas-phase  $\text{CO}_2$ . The background signal from gas-phase  $\text{CO}_2$  could be subtracted

successfully. The asymmetric stretching vibration of adsorbed  $\text{CO}_2$  occurred at  $2333\ \text{cm}^{-1}$ ,  $15\ \text{cm}^{-1}$  below the gas-phase value. It was accompanied by a weak shoulder at about  $2324\ \text{cm}^{-1}$ . The relative intensity of the lower frequency shoulder remained constant independent of  $\text{CO}_2$  loading (see the Supporting Information for the spectra). Switching to pure He resulted in a rapid decrease of the adsorbed  $\text{CO}_2$  signal to 1% of its original value within 2 minutes, indicating rapid diffusion within the MOF. This was confirmed by zero length column experiments on a 13 mg sample, which followed desorption of  $\text{CO}_2$  from a thin wafer of powder. These showed that desorption is 99% complete within a few tens of seconds at the flow rates used in the IR experiment (see the Supporting Information for details). Analysis shows that although the desorption is too fast to permit calculation of the diffusional time constant, an upper bound of  $R^2/D$  of 5.3 s can be estimated,<sup>[13]</sup> corresponding to a lower limit for diffusivity along the channels, *D*, of  $3 \times 10^{-10}\ \text{m}^2\text{s}^{-1}$ , higher than measured by different methods for zeolite 5A.<sup>[14]</sup>

In the light of this, an experiment was conducted in which spectra were measured on the selected crystal sites in the presence of 10%  $\text{CO}_2$  as the temperature was raised stepwise from 298 to 393 K. The sample was allowed to equilibrate for approximately 5 minutes at each temperature before unpolarized IR spectra were collected. As the temperature was increased the magnitude of the adsorbed  $\text{CO}_2$  asymmetric stretch decreased relative to the size of the peaks associated with the  $\text{NH}_2$  stretches (see Figure 2 for a series of spectra from a single point). This indicates that the concentration of adsorbed  $\text{CO}_2$  decreases with increasing temperatures, as expected for exothermic adsorption. Subsequently, similar series of experiments were performed as the partial pressure of  $\text{CO}_2$  was adjusted to 0.025, 0.050, and 0.2 bar. Above this pressure the absorption from gas-phase  $\text{CO}_2$  precluded accurate measurement.

IR spectra were analyzed using the OPUS 7.2 software.<sup>[15]</sup> Integrals were calculated for the  $\text{NH}_2$  symmetric and asym-

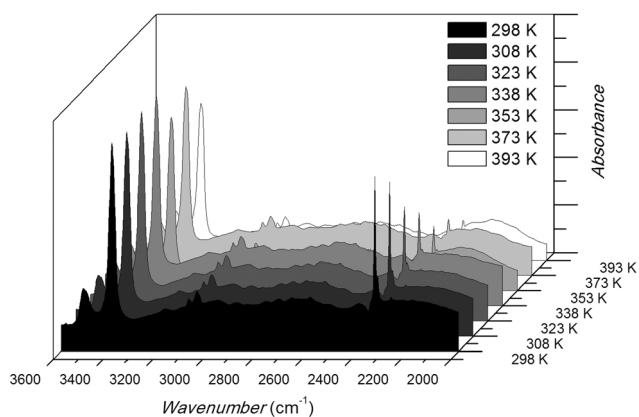


**Figure 2.** Series of spectra taken from an isobar from a single site of a single  $\text{Sc}_2(\text{BDC-NH}_2)_3$  crystal. As temperature increases the magnitude of the adsorbed  $\text{CO}_2$  asymmetric stretch at  $2335\text{ cm}^{-1}$  wavenumbers decreases relative to the  $\text{NH}_2$  symmetric and asymmetric stretches.

metric stretches and the  $\text{CO}_2$  asymmetric stretch. The combined integral associated with the  $\text{NH}_2$  stretches was used as an internal reference to quantify the uptake of  $\text{CO}_2$ , by calculating the ratio of the integral of the  $\text{CO}_2$  asymmetric stretch to that of the  $\text{NH}_2$  region. At 100 mbar  $\text{CO}_2$  and 298 K the specific uptake of  $\text{CO}_2$  on  $\text{Sc}_2(\text{BDC-NH}_2)_3$  was known from gravimetric measurements to be  $0.393\text{ mmol g}^{-1}$ . Measured peak area ratios were used to estimate the uptakes at each temperature in each isobar. Figure 3a shows the calculated uptake at 0.1 bar on the single crystal shown in Figure 1c. The variation of the uptakes at 0.1 bar measured by IR spectroscopy on single crystals and from gravimetric isotherms (see the Supporting Information) shows good agreement. Figure 3b shows the uptake from several crystals for isobars at 0.025, 0.05, 0.1, and 0.2 bar  $\text{CO}_2$ .

The uptakes were used to calculate a fractional coverage and hence a value for the equilibrium constant  $K$  for adsorption according to the equilibrium,  $\text{CO}_2(\text{g}) + \text{S} \leftrightarrow \text{CO}_2(\text{ads})$ , where S is the adsorption site. Full coverage was taken as  $5.1\text{ mmol g}^{-1}$ .<sup>[9]</sup> The heat of adsorption for  $\text{CO}_2$  in  $\text{Sc}_2(\text{BDC-NH}_2)_3$  was calculated using these single-crystal data to be  $31 \pm 2\text{ kJ mol}^{-1}$  from plots of  $\ln K$  vs.  $1/T$  (see the Supporting Information). This agrees with the isosteric heats calculated from a series of adsorption isotherms at different temperatures, the average of which was  $31 \pm 3\text{ kJ mol}^{-1}$ . The heats of adsorption on the amino-functionalized material are higher than those reported previously on  $\text{Sc}_2\text{BDC}_3$  ( $23\text{ kJ mol}^{-1}$ ).<sup>[16]</sup> This is the result of interactions of  $\text{CO}_2$  with  $\text{NH}_2$ .

IR spectroscopy can also be sensitive (in terms of frequency shifts) to molecular interactions. Upon  $\text{CO}_2$  adsorption on  $\text{Sc}_2(\text{BDC-NH}_2)_3$  the peak maxima for the symmetric and asymmetric  $\text{NH}_2$  stretches shift by approximately  $5\text{ cm}^{-1}$  to lower values ( $3396$  to  $3392\text{ cm}^{-1}$ ;  $3513$  to  $3508\text{ cm}^{-1}$ , respectively) suggesting a weak additional interaction between the  $\text{NH}_2$  groups and  $\text{CO}_2$ .

It is therefore possible to determine the rates, heat, and nature of adsorption of  $\text{CO}_2$  on single crystals using IR microspectroscopy under realistic conditions. While these could be obtained from bulk samples, the microscopic

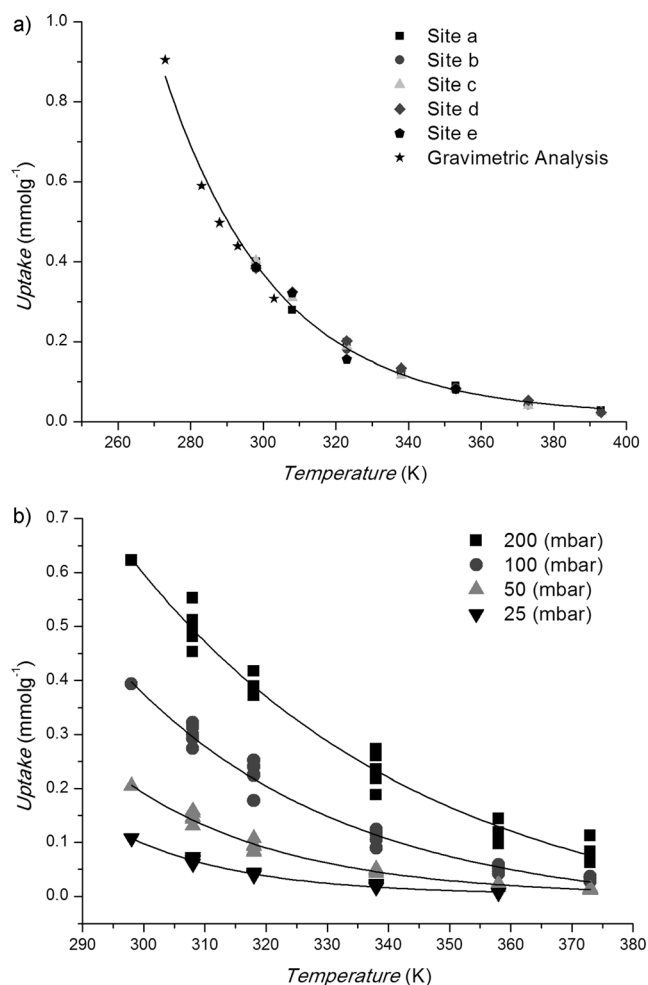


**Figure 3.** a)  $\text{CO}_2$  isobar ( $P_{\text{CO}_2} = 0.1\text{ bar}$ ), measured on 5 sites (Figure 1c) on a single crystal at 298–393 K (square, site a; circle, b; triangle, c; diamond, d; pentagon, e). Comparison between uptakes from single crystal IR data and conventional gravimetric adsorption (stars), fitted by an exponential curve calculated assuming a heat of adsorption of  $31\text{ kJ mol}^{-1}$ . b)  $\text{CO}_2$  isobars ( $P_{\text{CO}_2} = 25, 50, 100, 200\text{ mbar}$ ).

approach can measure variation between different crystals. Furthermore, and importantly, synchrotron IR single-crystal microspectroscopy can give information inaccessible to bulk methods, in particular by the use of a polarized IR beam.

To understand the adsorption of  $\text{CO}_2$  onto the MOF, non-polarized and polarized IR spectra were collected from crystals orientated parallel or perpendicular to the holographic ZnSe wire grid polarizers used to define the electric field direction of the IR beam being detected. The crystals of  $\text{Sc}_2(\text{BDC-NH}_2)_3$  have well-defined facets, so that it is possible from the optical image to establish the crystal orientation with respect to the polarized beam: crystals were found to settle in one of three ways: with their (001), (011) or (010) plane parallel to the window (and perpendicular to the plane of the polarized IR light). Schematic representations of these orientations (illustrated by SEM micrographs) are shown in Figure 4. Spectra were collected at 298 K using unpolarized IR light and also IR light polarized parallel and perpendicular

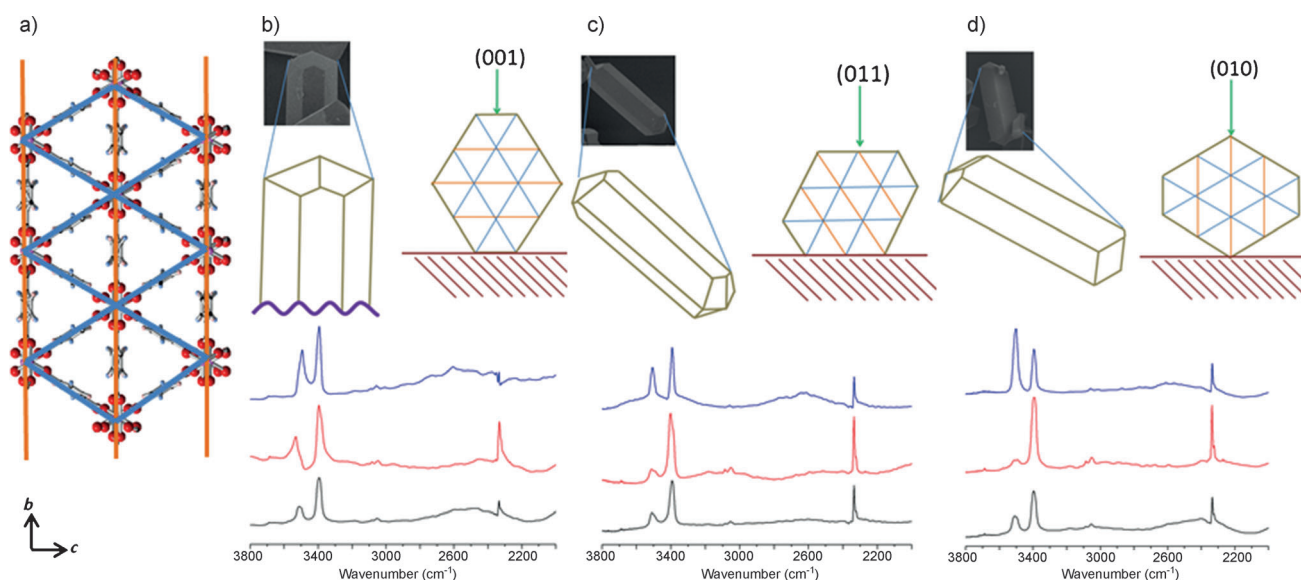


**Figure 4.** a) The framework of  $\text{Sc}_2(\text{BDC-NH}_2)_3$  viewed down the  $a$  axis, which corresponds to the morphologically longest direction of the crystals. Orange (type 1 linker) and blue (type 2 linker) lines indicate the projections of the different linkers. b,c,d) Scanning electron micrographs of crystals in similar orientations to those studied, and schematic representations, for crystals lying with (001), (011) and (010) planes parallel to the window of the cell, respectively. The spectra (b,c,d) are of unpolarized spectra of the MOF with adsorbed  $\text{CO}_2$  (black), spectra with direction of polarization parallel (red) and perpendicular (blue) to long morphological axis of a crystal lying on (001), (011), and (010) faces, respectively.

to the crystal length, on activated crystals and in 0.1 bar  $\text{CO}_2$ . Integrals were calculated for the  $\text{NH}_2$  symmetric and the  $\text{CO}_2$  asymmetric stretches, to enable details of the orientation of adsorbed molecules in the functionalized framework to be measured (see the Supporting Information).

In each case the polarized FTIR spectra reveal that the absorbance of the  $\text{NH}_2$  symmetric stretch increases when the polarization is parallel to the long direction of the crystal, indicating that the  $\text{C}_{\text{ph}}-\text{N}$  bonds aligned along the channels. Very similar  $\text{NH}_2$  absorbance behavior is observed in crystals with and without adsorbed  $\text{CO}_2$ , suggesting that there is no significant re-orientation of the ligands upon uptake of  $\text{CO}_2$ . Furthermore, the  $\text{CO}_2$  asymmetric stretch intensity is enhanced when the IR light is polarized along the crystal length, indicating that the average alignment of the  $\text{CO}_2$  molecules is oriented along the channels.

A more quantitative estimation of the  $\text{CO}_2$  alignment can be made if the structure of  $\text{Sc}_2(\text{BDC-NH}_2)_3$  is considered (Figure 1d and Figure 4). Intensities of polarized SR IR spectra vary strongly according to orientation, but by comparing the relative enhancement or suppression of the  $\text{CO}_2$  asymmetric stretch with respect to the symmetric  $\text{NH}_2$  stretch (which is expected to give a dipole change parallel to the  $\text{C}_{\text{ph}}-\text{N}$  bond) it is possible for each of the projections to determine whether the  $\text{CO}_2$  molecules are aligned more or less closely to the channel axis than the net  $\text{C}_{\text{ph}}-\text{N}$  vector. (It is not possible to locate the amine hydrogen atoms by diffraction, so we have not analyzed directional information from the asymmetric stretch.) The  $\text{C}_{\text{ph}}-\text{N}$  vectors for all of the possible orientations of amino groups on the terephthalate ligands were measured from projections of the single-crystal structure down [001], [011] and [010], and a weighted average of their deviation from the [100] axis was determined (see the

Supporting Information). The net  $\text{C}_{\text{ph}}-\text{N}$  vector is close to parallel to the channel axis in the MOF ( $17^\circ$  off-parallel viewed down [001],  $13^\circ$  off-parallel viewed down [011], and  $11^\circ$  off-parallel for [010]). The intensity of the asymmetric stretch of the linear  $\text{O}=\text{C}=\text{O}$  molecule is enhanced relative to the  $\text{NH}_2$  symmetric stretch using IR light polarized along the crystal length when viewed down [001] (by ca. 90%) and [011] (by 23%) but is suppressed when viewed down [010] (by 17%). The projection of the  $\text{CO}_2$  molecule is therefore more closely aligned to the channel axis than  $17^\circ$  when viewed down [001] and makes a larger angle than  $11^\circ$  when viewed down [010], in effect enabling triangulation of the relative orientation of the  $\text{CO}_2$  molecules' orientation in the channel, which is on average closer than approximately  $20^\circ$  to the channel axis.

A powerful new SR FTIR microspectroscopic technique has been developed which permits the rapid analysis of adsorption by porous materials under flowing gas conditions relevant to carbon capture. Investigations on an amino-functionalized MOF give a heat of adsorption and desorption rates on a single crystal and polarized IR light has been used to show a strong orientation dependency of adsorbed  $\text{CO}_2$  molecules within the pores of  $\text{Sc}_2(\text{BDC-NH}_2)_3$ , even at rather low uptakes, a result which is experimentally difficult to attain by other means. Whereas previous diffraction measurements have located adsorbed  $\text{CO}_2$  on MOFs at room temperature at loadings down to approximately  $1 \text{ mmol g}^{-1}$ ,<sup>[17]</sup> these IR measurements give acceptable signal-to-noise ratios for the asymmetric stretch of adsorbed  $\text{CO}_2$  at  $< 0.1 \text{ mmol g}^{-1}$  (fractional site occupancies  $< 0.015$ ). Furthermore, the method has the potential to follow temporal and spatial variation over a single crystal and so to determine adsorbate diffusivities. Although the diffusion of  $\text{CO}_2$  in  $\text{Sc}_2(\text{BDC-NH}_2)_3$  is too fast to

permit this, there are many examples of more slowly diffusing, IR-active molecules (e.g. H<sub>2</sub>O, N<sub>2</sub>O, small hydrocarbons or organics) in other porous solids than can be studied in this way, even when part of adsorbing mixtures, especially when developments in full field FTIR imaging using synchrotron radiation IR brilliance can offer faster acquisition and a larger field of view (see the Supporting Information).<sup>[18]</sup>

The results reported here confirm the potential of amino-functionalized MOFs as carbon capture materials and indicate that in situ single-crystal gas adsorption and polarized IR microspectroscopy can rapidly provide unique insights into single- and eventually multi-component adsorption processes.

Received: August 19, 2014

Published online: November 7, 2014

**Keywords:** analytical methods · carbon dioxide adsorption · IR spectroscopy · metal–organic frameworks · single crystals

- 
- [1] K. Sumida, D. L. Rogow, J. A. Mason, T. M. McDonald, E. D. Bloch, Z. R. Herm, T. H. Bae, J. R. Long, *Chem. Rev.* **2012**, *112*, 724–781.
- [2] a) B. Li, S. S. Kaye, C. Riley, D. Greenberg, D. Galang, M. S. Bailey, *ACS Comb. Sci.* **2012**, *14*, 352–358; b) T. H. Bae, M. R. Hudson, J. A. Mason, W. L. Queen, J. J. Dutton, K. Sumida, K. J. Micklash, S. S. Kaye, C. M. Brown, J. R. Long, *Energy Environ. Sci.* **2013**, *6*, 128–138.
- [3] N. Nijem, P. Canepa, L. Kong, H. Wu, J. Li, T. Thonhauser, Y. J. Chabal, *J. Phys. Condens. Matter* **2012**, *24*, 424203.
- [4] C. O. Areal, G. F. Babiloni, M. R. Delgado, *Appl. Surf. Sci.* **2012**, *259*, 367–370.
- [5] P. L. Llewellyn, S. Bourelly, C. Vagner, N. Heymans, H. Leclerc, A. Ghoufi, P. Bazin, A. Vimont, M. Daturi, T. Devic, C. Serre, G. De Weireld, G. Maurin, *J. Phys. Chem. C* **2013**, *117*, 962–970.
- [6] M. M. Lozinska, E. Mangano, J. P. S. Mowat, A. M. Shepherd, R. F. Howe, S. P. Thompson, J. E. Parker, S. Brandani, P. A. Wright, *J. Am. Chem. Soc.* **2012**, *134*, 17628–17642.
- [7] a) C. Chmelik, J. Kärger, *Chem. Soc. Rev.* **2010**, *39*, 4864–4884; b) J. Kärger, T. Binder, C. Chmelik, F. Hibbe, H. Krautscheid, R. Krishna, J. Weitkamp, *Nat. Mater.* **2014**, *13*, 333–343.
- [8] E. Pantatosaki, G. Megariotis, A.-K. Pusch, C. Chmelik, F. Stallmach, G. K. Papadopoulos, *J. Phys. Chem. C* **2012**, *116*, 201–207.
- [9] J. P. S. Mowat, S. R. Miller, J. M. Griffin, V. R. Seymour, S. E. Ashbrook, S. P. Thompson, D. Fairen-Jimenez, A.-M. Banu, T. Düren, P. A. Wright, *Inorg. Chem.* **2011**, *50*, 10844–10858.
- [10] E. Stavitski, B. M. Weckhuysen, *Chem. Soc. Rev.* **2010**, *39*, 4615–4625.
- [11] F. Schüth, D. Demuth, B. Zibrowius, J. Kornatowski, G. Finger, *J. Am. Chem. Soc.* **1994**, *116*, 1090–1095.
- [12] E. C. V. Eschenroeder, A. Turrina, A. L. Picone, G. Cinque, M. D. Frogley, P. A. Cox, R. F. Howe, P. A. Wright, *Chem. Mater.* **2014**, *26*, 1434–1441.
- [13] S. Brandani, D. M. Ruthven, *Adsorption* **1996**, *2*, 133–143.
- [14] a) D. M. Ruthven, *Zeolites* **1993**, *13*, 594; b) J. Kärger, H. Pfeifer, F. Stallmach, N. Feoktistova, S. P. Zhdanov, *Zeolites* **1993**, *13*, 50–55.
- [15] OPUS software 7.0, Bruker Optik GmbH, Germany, **2011**
- [16] S. R. Miller, P. A. Wright, T. Devic, C. Serre, G. Férey, P. L. Llewellyn, R. Denoyel, L. Gaberova, Y. Filinchuck, *Langmuir* **2009**, *25*, 3618–3626.
- [17] M. Wriedt, J. P. Sculley, A. A. Yakovenko, Y. Ma, G. J. Halder, P. B. Balbuena, H.-C. Zhou, *Angew. Chem. Int. Ed.* **2012**, *51*, 9804–9808; *Angew. Chem.* **2012**, *124*, 9942–9946.
- [18] L. Quaroni, T. Zlateva, B. Sarafimov, H. W. Kreuzer, K. Wehbe, E. L. Hegg, G. Cinque, *Biophys. Chem.* **2014**, *189*, 40–48.
-